

TOPOLOGY MEETS MACHINE LEARNING: AN INTRODUCTION USING THE EULER CHARACTERISTIC TRANSFORM

BASTIAN RIECK

Department of Computer Science, University of Fribourg, Switzerland

Machine learning is shaping up to be *the* transformative technology of our times: Many of us have played with (and marveled at) models like ChatGPT, new breakthroughs in applications like healthcare research are announced on an almost daily basis, and new avenues for integrating these tools into scientific research are opening up, with some mathematicians already using large language models as proof assistants.

This article aims to lift the veil and dispel some myths about machine learning; along the way, it will also show how machine learning itself can benefit from mathematical concepts. Indeed, from the outside, machine learning might look like a homogeneous entity, but in fact, the field is fractured and highly diverse. While the main thrust of the field arises from the undeniable engineering advances, with bigger and better models, there is also a strong community of applied mathematicians. Next to the classical drivers of machine-learning architectures, i.e., linear algebra and statistics, *topology* recently started to provide novel insights into the foundations of machine learning: *Point-set topology*, harnessing concepts like neighborhoods, can be used to extend existing algorithms from graphs to cell complexes [4]. *Algebraic topology*, making use of effective invariants like homology, improves the results of models for volume reconstruction [13]. Finally, *differential topology*, providing tools to study smooth properties of data, results in efficient methods for analyzing embedded (simplicial) complexes [6]. These (and many more) methods have now found a home in the nascent field of *topological deep learning* [8]. Before diving into concrete examples, let us first take a step back and discuss machine learning as such.

1. What is Machine Learning?

Machine learning is broadly construed as the art and science of employing algorithms to solve tasks, but with the added restriction that the algorithm should—in a certain sense that will become clear below—adapt itself to the data at hand. To substantiate this definition, we need to introduce some terms that often arise in machine-learning research. We start with the notion of a *feature*, which is arguably central to machine-learning algorithms. A feature refers to a quantity derived from “raw” input data. For instance, given a set of chemical structures, we can define a feature as the number of carbon atoms. Adding other features—such as the number of oxygen atoms, ring structures, or aromatic bounds—then yields a high-dimensional representation of a chemical structure in the form of a *feature vector*, which, for convenience, we assume to live in some \mathbb{R}^d .

Machine-learning algorithms may thus, on a very high level, be seen as functions of the form $f : \mathbb{R}^d \rightarrow \mathcal{D}$, where \mathcal{D} indicates some domain of interest. For instance, suppose we are interested in classifying chemical structures into different classes, the domain \mathcal{D} could consist

E-mail address: bastian.grossenbacher@unifr.ch.

of the labels “toxic” and “harmless.” Such a task is also known as *supervised machine learning*.¹ Not every function f is equally useful, though, in this context. If f would always predict “toxic,” it would not be a suitable function for our task (even though its prediction might be the safest bet). The allure of machine learning lies in the fact that it provides a framework to *learn* a suitable function f by presenting the algorithm with numerous examples of different structures, in the hope that with sufficient data, the underlying mechanism driving toxicity can be derived. Thus, when we show this function a new example, its guess as to whether it is toxic or not is based on all previously-seen examples. Machine learning knows many suitable algorithms that enable the creation of such functions. Chief among those is the concept of *deep learning* or *deep neural networks*.² Deep-learning models started a veritable revolution in some fields like computer vision, mostly because (i) they obviate the need for “hand-crafted” features, as introduced at the beginning of this section, and (ii) they consist of standalone building blocks, i.e., *layers*, that can be easily combined to build new models for solving domain-specific problems.

Initially, all layers of a deep neural network start with a random set of parameters or *weights*, which are then subsequently adjusted to minimize a *loss function*. For our running example, *binary cross-entropy* (BCE) is a suitable loss function. Mapping {“non-toxic,” “toxic”} to {0, 1}, the BCE loss for n predictions is

$$(1) \quad \frac{1}{n} \sum_{i=1}^n y_i \log(p_i) + (1 - y_i) \log(1 - p_i),$$

where $y_i \in \{0, 1\}$ represents the true label of a sample and $p_i \in [0, 1]$ refers to the prediction of the neural network, which we assume to denote the probability³ of the sample being in class 1, i.e., being toxic. The parameters of the neural network are now subsequently adjusted, with the goal of minimizing Eq. (1). To this end, we repeatedly perform the prediction for a set of predefined samples, the so-called *training data set*, which is presented to the neural network in equal-sized *batches* (as opposed to using the full data set as an input, which would often be prohibitive in terms of memory requirements). Once we are satisfied with the results, we evaluate the prediction on the *test data set*, which crucially, must be kept separate from the training data set.

A common dismissal of deep learning is that it “just” performs curve-fitting, arguably in a highly-elaborate way. While this article cannot possibly counter all such arguments, it should be pointed out that (some) neural networks can approximate certain function spaces arbitrarily well. This property is also known as *universal function approximation* and implies that a certain class of neural networks is dense in some function space. For instance, feedforward neural networks are known to be able to approximate any Borel-measurable function between finite-dimensional spaces [5]. Similar theorems exist for other architectures and this property is often invoked when discussing the merits of deep learning. A deep neural network with sufficient data might be the easiest way to approximate functions that do not permit analytical solutions.

The conceptual simplicity and modularity of deep neural networks is not without its downsides, though. To perform well, deep neural networks typically require enormous amounts of data as well as a humongous number of parameters. Unless specific provisions are taken, deep neural networks are not energy-efficient, and their data requirements still pose serious obstacles in many domains. In addition, neural networks are still black-box models with opaque outputs. Even though research in *interpretable machine learning* is improving this state of affairs, there are still few models whose outputs can be easily checked by human operators, for instance. Even *large language models* (LLMs), arguably one of the most impressive feats of the field, suffer from shortcomings and are incapable of assessing their own outputs. Like other deep neural networks, they also remain vulnerable to *adversarial attacks*, i.e., inputs that are

¹In *unsupervised machine learning*, by contrast, input data are not labeled, requiring models to “learn” characteristic properties of the data-generation process such as clusters.

²See Schmidhuber [10] for a “deep dive” into the respective algorithms and their origin stories.

³In practice, the result of log is *clamped* to a finite range to ensure that gradients are always well-defined.

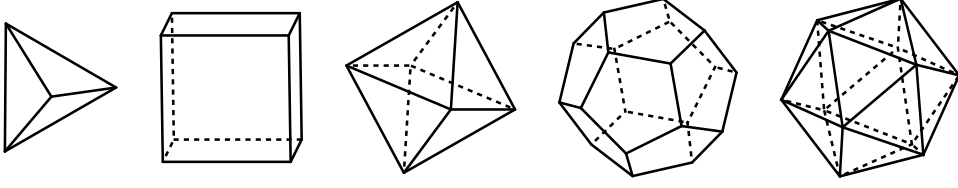


Figure 1. The five platonic solids, i.e., a tetrahedron, a cube, an octahedron, a dodecahedron, and an icosahedron. Their Euler characteristic is 2.

Table 1. Vertex, edge, and face counts for each of the platonic solids shown in Figure 1.

<i>Polyhedron</i>	No. vertices	No. edges	No. faces
Tetrahedron	4	6	4
Cube	8	12	6
Octahedron	6	12	8
Dodecahedron	20	30	12
Icosahedron	12	30	20

generated to provoke a bad response, often without the original user of the model being aware of it. Adversarial examples for vision models can appear innocuous to a human observer but can cause incorrect predictions: Traffic signs can be slightly remodeled using adhesive tape, making a vision system being unable to detect them, for example. Deep learning thus still offers fundamental challenges that necessitate an analysis of its very foundations. It is here that topology can provide a new perspective.

2. Euler Characteristic Galore

We focus our discussion on the *Euler Characteristic Transform* (ECT). Being an invariant that bridges geometry and topology, it is perfectly suited for such an overview article because it hopefully provides connection points for the largest amount of researchers. The ECT is based on the concept of an *Euler Characteristic*. This integer-based quantity serves as a summary statistic of the “shape” of a graph or simplicial complex. For a p -dimensional simplicial complex K , the Euler Characteristic is defined as

$$(2) \quad \chi(K) := \sum_{i=0}^p (-1)^i |K_i|,$$

i.e., an alternating sum of the cardinalities of the i -skeletons K_i of K . The Euler characteristic is marvelous in that it affords several equivalent definitions (for instance, in terms of the Betti numbers of K) and can be assigned to different objects. Moreover, it is a *topological invariant*, meaning that if two spaces (objects) are homotopy-equivalent, their Euler characteristic is the same. This is depicted in Figure 1 and Table 1 by means of the classical example of the five platonic solids. Being homotopy-equivalent to \mathbb{S}^2 , the 2-sphere, their Euler characteristic is the same.

While the single number $\chi(K)$ does not carry sufficient expressivity to fully characterize all shapes, it is possible to lift it to a multi-scale summary known as the *Euler Characteristic Transform* (ECT), which turns out to be an *injective* map into the space of all shapes [11]. The ECT requires an embedded simplicial complex K in \mathbb{R}^d . We can think of such a complex to have an associated coordinate x_v for each vertex v of a simplex σ . Taking now any direction $w \in \mathbb{S}^{d-1}$, i.e., any point on the $(d-1)$ -sphere with unit radius, we obtain a real-valued function defined

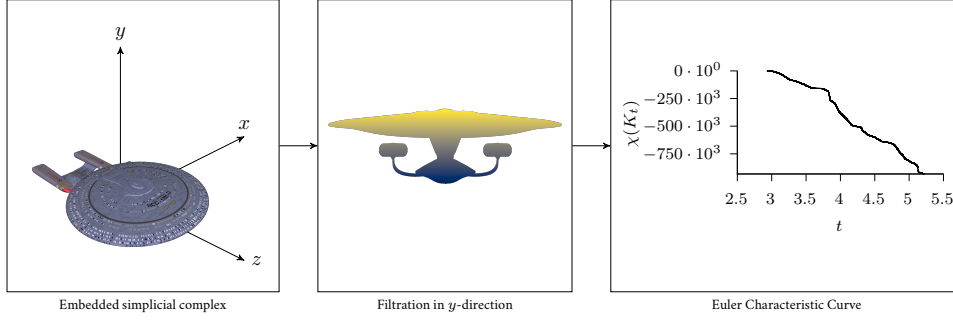


Figure 2. An illustration of the Euler Characteristic Curve calculation procedure. Starting from a 3D model, specified as a *mesh* with vertex, edges, and faces, we perform a single filtration in the direction of the y -axis. The filtration values are shown in the cross-section of the model, with warmer colors corresponding to larger filtration values. Finally, the Euler Characteristic Curve is plotted for all thresholds.

for all simplices of K via

$$(3) \quad \begin{aligned} f: K &\rightarrow \mathbb{R} \\ \sigma &\mapsto \max_{v \in \sigma} \langle x_v, w \rangle, \end{aligned}$$

where $\langle \cdot, \cdot \rangle$ denotes the standard Euclidean inner product. In the parlance of computational topology, this function f can be used to obtain a *filtration* of K in terms of its subcomplexes: Given a threshold $t \in \mathbb{R}$, we define $K_t := \{\sigma \in K \mid f(\sigma) \leq t\}$. Evaluating the Euler characteristic of each K_c then yields the *Euler Characteristic Curve* (ECC) associated to the direction w . The ECC is an integer-valued function of the form

$$(4) \quad \begin{aligned} \text{ECC}: \mathbb{S}^{d-1} \times \mathbb{R} &\rightarrow \mathbb{Z} \\ (w, t) &\mapsto \chi(K_t). \end{aligned}$$

The ECC thus maps a direction and a threshold to the Euler characteristic of the corresponding subcomplex. Figure 2 depicts the ECC calculation procedure for a *mesh*, i.e., an embedded simplicial complex with vertex coordinates in \mathbb{R}^3 .

With all the ingredients in place, we finally obtain the *Euler Characteristic Transform* (ECT) as the function that assigns each direction $w \in \mathbb{S}^{d-1}$ to the corresponding ECC. Thus,

$$(5) \quad \begin{aligned} \text{ECT}: \mathbb{S}^{d-1} &\rightarrow \mathbb{Z}^{\mathbb{R}} \\ w &\mapsto \text{ECC}(w, \cdot), \end{aligned}$$

where $\mathbb{Z}^{\mathbb{R}}$ denotes the set of functions from \mathbb{Z} to \mathbb{R} . Turner et al. [11] introduced the ECT and proved that it serves as a sufficient shape statistic if an infinite number of directions is used. This result alone is already surprising, but later on, Curry et al. even showed that a finite number of directions is sufficient in practice [3]. Intuitively, this is similar to how a sufficiently large number of 2D images often lets us reconstruct 3D volume data. To learn more about the ECT, the reader is strongly recommended to check out an excellent overview article by Munch [7].

3. Using the Euler Characteristic Transform in a Machine-Learning Model

Given its surprising properties in bridging geometrical and topological aspects of data, integrating the ECT into machine-learning models seems to be almost the next logical step. But before we discuss how to use the ECT with a deep-learning model, let us first ponder some of

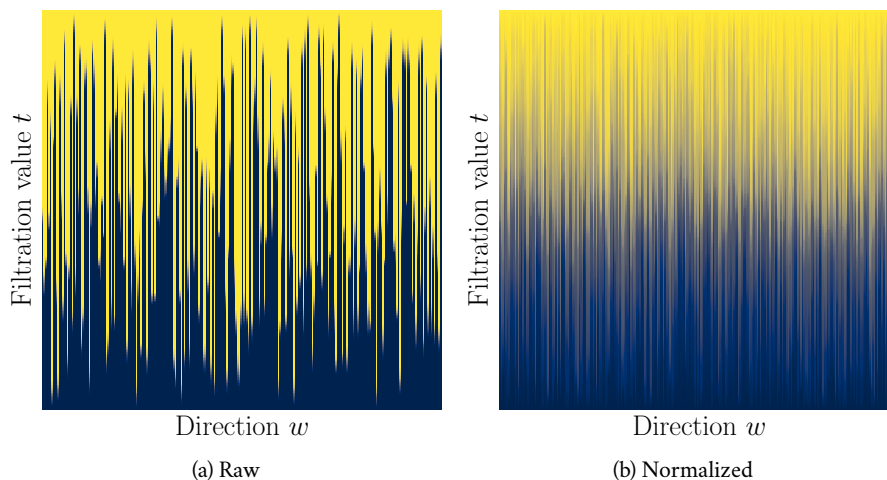


Figure 3. Visualizing the ECT of the model in Figure 2 as a discretized image using either the raw t -values (left), or a re-scaled version (right) with $t \in [-1, 1]$. Each x -axis shows 256 randomly-selected directions, while each y -axis corresponds to the filtration values t , with the lowest value starting at the top of the image. Every column in the image corresponds to an individual ECT, with the pixel color indicating the value for a specific filtration threshold t . Warmer colors correspond to larger ECT values.

its practical uses with classical⁴ machine-learning methods like *support vector machines*. Central to such algorithms is their use of hand-crafted features; while often eschewed in deep learning, the power of such features should not be underestimated—in particular when combined with methods like the ECT.

Given the results by Curry et al. [3], there is some utility in only using a finite set of directions to calculate the ECT. In practice, however, it is unclear how to find such directions. This leads researchers to sample a set of directions $W := \{w_1, \dots, w_k\} \subset \mathbb{S}^{d-1}$, and consider the ECT restricted to W . The hope is that the sample is sufficient to capture shape characteristics. Another discretization applied in practice involves the choice of thresholds. For example, if each associated coordinate of x_v has at most unit norm, we know that $\langle x_v, w \rangle \in [-1, 1]$. Thus, in practice, we could sample thresholds $T := \{t_1, \dots, t_l\} \subset [-1, 1]$ and evaluate each ECC for a specific direction w only at thresholds in T . The result is that we can represent the ECT as a matrix, where columns are indexed by W and rows are indexed by T . Equivalently, this matrix can be viewed as an *image*, although the ordering of directions, i.e., the columns of the matrix/image, is arbitrary. Figure 3 depicts this visualization for 256 randomly-selected directions. In contrast to the normalized version, the use of “raw” values of t to index the rows results in more zeros. This is a consequence of the fact that individual columns, i.e., ECCs are not aligned to the same domain. At the same time, the lack of normalization permits interpreting differences between columns, whereas in the normalized version, such differences need to be understood relative to the specific values of (t, w) .

Setting aside the dissimilarities between the two variants, it is possible to compare shapes by calculating an appropriate distance between their respective ECT images. Such approaches work best when shapes are canonically aligned to a shared coordinate system [1]. An alternative to this involves “flattening” the matrix, thus effectively turning the matrix into a long feature vector. Similar to our initial example with chemical structures, this process enables us to represent a complex shape as a fixed-size vector. Such a representation depends crucially on

⁴While this is the common nomenclature as used in the machine-learning community, it should be pointed out that some of these methods predate deep learning by a couple of years only. This indicates the rapid pace of the field.

the choices of thresholds and directions, but is seen to lead to good results in practice. An interesting question is whether we can move beyond such hand-crafted features. While some discretization is unavoidable, a different way of representing the ECT would ideally enable us to *learn* an appropriate set of directions W as opposed to *sampling* it. This would obviate the need for sampling a set of fixed directions. One obstacle to overcome here involves the fact that the ECT is a discrete quantity based on step functions. Such functions are at odds with deep-learning models, who prefer things to be smooth and differentiable. One option could be to consider the smooth ECT, obtained from the ECT by mean-centering and integration [2]. Another option uses a trick often found in machine-learning research: Instead of working with the original definition of a function, we just work with a smooth approximation to it! While this technically solves a different problem than what we originally set out to achieve, it often works surprisingly well; the so-called *Gumbel-max trick*, for instance, is commonly employed when having to deal with categorical (as opposed to continuous) distributions. Regardless of the specific approximation method, this procedure will permit us to use the ECT to affect the assumptions that are used by a model to obtain its predictions. The ECT may thus be said to constitute an *inductive bias*.

In the spirit of approximating the ECT, we first notice that any ECC can be written as a sum of *indicator functions*, i.e., we rewrite Eq. (4) as

$$(6) \quad \begin{aligned} \text{ECC}: \mathbb{S}^{d-1} \times \mathbb{R} &\rightarrow \mathbb{Z} \\ (w, t) &\mapsto \sum_{i=0}^p (-1)^i \sum_{\sigma \in K_t^{(i)}} \mathbb{1}_{\leq t}(f(\sigma)), \end{aligned}$$

where $K_t^{(i)}$ denotes the i -skeleton of K_t , and f refers to the filtration from Eq. (3). Equivalently, Eq. (5) permits a rephrasing via indicator functions. So far, this is still an exact expression. The approximation comes into play when we notice that an indicator function can be replaced by a *sigmoid function*, i.e., $S(x) = 1/(1+e^{-x})$. This lets us define an approximate ECC by rewriting Eq. (6) via

$$(7) \quad (w, t) \mapsto \sum_{i=0}^p (-1)^i \sum_{\sigma \in K_t^{(i)}} S(\lambda(h - f(\sigma))),$$

where $\lambda \in \mathbb{R}$ denotes a scaling parameter that controls the tightness of the approximation. Figure 4 depicts this approximation for various values; we can see that $S(\lambda x)$ is indeed a suitable (smooth) replacement for an indicator function. This minor modification has major advantages: *Each* of the summands in Eq. (7) is differentiable with respect to w , t , and $f(\cdot)$. It is thus possible to use Eq. (7) to transform an embedded simplicial complex in a way that is fundamentally compatible with a deep-learning model.

Lest we get lost in implementation details, it is better to assume a more elevated position and take stock of what we already have: Using the approximation above, we have turned the ECT from a discrete function into a function that *continuously* depends on its input parameters. In machine-learning terminology, we may thus treat this calculation as a *layer*. Assuming that all coordinates have at most unit norm so that $\langle x_v, w \rangle \in [-1, 1]$, our ECT layer has two hyperparameters, namely (i) the number l of thresholds to use to discretize $[-1, 1]$, and (ii) the number k of directions to use. Thus, the input of the layer is an embedded simplicial complex K , and the output of the layer is a $l \times k$ matrix (equivalently, we may apply such a construction to all types of spaces that afford an Euler Characteristic, including *cell complexes*, for instance). Notice that when learning an ECT for a data set of different objects, one matrix (i.e., the discretized image of an ECT) for each sample in the input batch is returned, resulting in a multidimensional array output, which, is also referred to as a *tensor*.⁵ Given the continuous

⁵This terminology can be confusing for mathematicians at first since machine learning does not (always) make use of any of the properties that would make up a “mathematical” tensor.

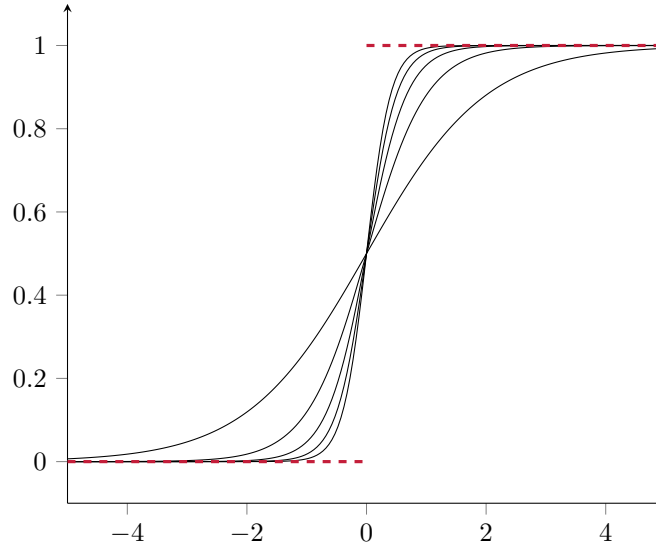


Figure 4. An indicator function (dashed) and its approximation using differently-scaled sigmoid functions, with $\lambda \in \{1, 2, 3, 4, 5\}$.

dependence on its input parameters, we thus refer to the construction above as the *Differentiable Euler Characteristic Transform* [9].

4. Two Applications of Differentiable Euler Characteristic Transforms

The ECT layer we defined above gives rise to a fixed-size vectorial representation, which may either be integrated into a larger neural network—thus effectively handing off the ECT results for deeper processing—or which can be used directly on its own. As an example of the latter case, we can for instance *compare* two outputs of an ECT layer using a loss function. Treating the outputs as high-dimensional vectors x and y , we can use the squared l^2 -norm of their difference as a criterion of how well they are aligned. This loss function is also known as the *mean squared error* (MSE) loss function. It is commonly used to solve problems in *representation learning*, so it is perfectly suited for a small experiment: Suppose we have a simple data set in \mathbb{R}^2 whose (discretized) ECT we know. Starting from a randomly-initialized set of directions, can we *learn* the “best” directions that aligns the two ECTs? It turns out that the approximation scheme defined in Eq. (7) indeed permits solving such problems. Setting up a toy problem, we can start with 32 uniformly-sampled directions, which we can parametrize using a single angle (thereby even containing a canonical ordering). We then sample the same number of angles from a normal distribution and minimize the MSE loss between the ECT based on the random directions to the “original” ECT. Figure 5 depicts this experiment. After only a couple of optimization steps, we obtained a suitable approximation to our input ECT; this approximation gets better with longer training times and more discretization steps.

However, learning the directions could be considered somewhat solipsistic in that we derived a new representation (the ECT) and then showed that we can learn its parameters. Indeed, this experiment is more of a “smoke test,” since learning the parameters of a representation is the very basis of machine learning! To build a stronger experiment showcasing the power of the ECT, let us consider learning *coordinates* instead. Recall that our approximation from Figure 4 permits us to also affect the coordinates themselves: Any loss function that we evaluate will depend on the directions *and* the coordinates; thus, if we make the coordinates a parameter of our layer, we can modify them similarly to the example shown above. Using an MSE loss, this time we search for input coordinates that minimize the differences of our ECT to a target ECT (machine-learning researchers also like to use the term *ground truth*). Figure 6 depicts an

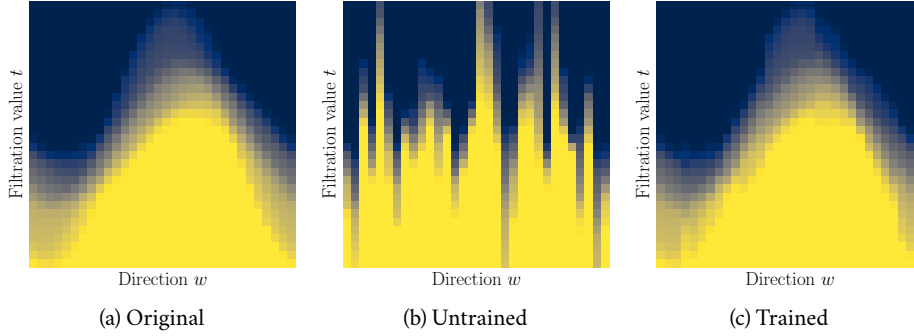


Figure 5. (a) We can learn the directions required to match the ECT of a simple data set. (b) Starting with a set of random directions, our initial “guess” of the ECT looks nothing like the original. (c) After several optimization steps, which minimize the dissimilarity between “our” ECT and the original one, we obtain a suitable approximation. We thus have learned a set of suitable directions for calculating the ECT.

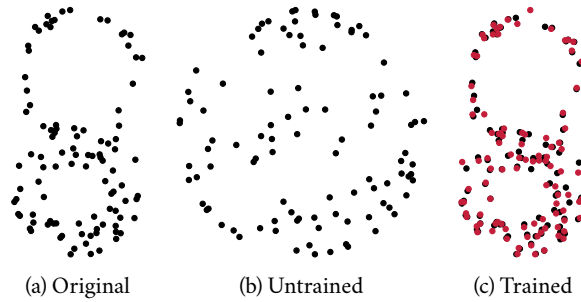


Figure 6. We can also learn the *coordinates* of a point cloud based on the ECT. (a) We sample 100 points from a double annulus. (b) The initial configuration of our coordinates is a random sample from a noisy circle. (c) After minimizing the coordinates based on measuring the dissimilarity between the “desired” ECT and the current one, we are able to approximate the input point cloud closely (red points show the learned coordinates, black points the original ones).

example, using $k = 256$ directions and $l = 256$. We again manage to quickly “learn” suitable coordinates to align our point cloud to the target point cloud.

These tasks demonstrate the versatility of the ECT. While learning directions or coordinates is not necessarily a machine-learning task *sui generis*, a computational layer based on the ECT permits us some flexibility; in conjunction with the loss term, we can employ the ECT in a variety of tasks. For instance, we can use it to classify *geometric graphs*, i.e., low-dimensional simplicial complexes whose vertices are embedded in some \mathbb{R}^n . This task is typically dominated by graph neural networks, which employ a mechanism called *message passing* that amounts to locally transporting information via the edges of a graph.⁶ The ECT offers a new and surprisingly competitive method for classifying such graphs. Together with its extremely small memory footprint—recall that the ECT is essentially “just” counting the constituent parts of an input object—this makes the ECT an interesting paradigm to consider for new machine-learning applications. Some of these applications are already discussed by Turner et al. [11], while others,

⁶An expository article like this cannot possibly do justice to the large body of research available under that moniker. The reader is therefore invited to consult a recent position paper for more details [12].

including the experiments for learning directions and coordinates, have been introduced in our recent work [9]. As always, there is much more work to be done, some enticing directions being (i) an assessment of the theoretical expressivity of the ECT when it comes to distinguishing between geometric graphs, (ii) the analysis of the *inverse problem*, i.e., the reconstruction of objects based on an ECT, in the discrete setting, and (iii) algorithmic aspects that enable the ECT to perform efficiently in the context of high-volume geometry-based streaming data arising from LiDAR sensors, for instance.

5. The Future of Topology in Machine Learning

A bright future in machine learning being virtually guaranteed for the ECT, let us briefly zoom out and consider the larger picture (knowing full well that predictions are hard, especially when concerning the future). By design, this article could merely scratch the surface, but the author firmly believes that topology and topological concepts have a strong role to play in machine learning. Many interesting directions are bound to fall into one of the following three areas:

- (1) Learning functions on topological spaces such as simplicial complexes or cell complexes.
- (2) Building hybrid models that imbue neural networks with knowledge about topological structures in the data.
- (3) Analyzing qualitative properties of neural networks.

In the first area, topology can be used to generalize existing machine-learning paradigms to a larger variety of input data set; this is appealing because not every data set “lives” in a nice Euclidean space or a graph, and the inclusion of higher-order neighborhoods would provide a shift in perspective, aiding knowledge discovery. As for the second area, researchers in *topological data analysis* (TDA) might feel particularly comfortable here since it is one of the declared aims of TDA to understand topological features in data. Nevertheless, hybrid models do not necessarily only have to draw upon concepts from TDA, despite the wealth of research already available here; new and daring methods could for instance focus on computational aspects of Riemannian geometry like curvature or make use of new invariants like metric-space magnitude. Finally, the third area shifts the perspective and lets topology return to its roots in that it can serve as a lens through which to study, for instance, the training behavior of neural networks. Understanding these training dynamics could lead to smaller, more efficient models, but also shed some light on the soft underbelly of deep-learning models, namely their susceptibility to unstable training regimens, “adversarial” input data, or their propensity for hallucinations.

Each of the three areas for new research has something enticing to offer, not only for machine learning but also for (applied) topology. There is vast potential for new topology-aware models to serve as proof assistants or even try to search for new conjectures and counterexamples. Thus, having hopefully aroused the reader’s interest in this matter, a recent position paper provides a suitable place to start one’s journey into this wonderful topic [8]. It is said that only those with their feet on rock can build castles in the air. Topology can provide this rock upon which robust machine-learning research can be built.

References

- [1] E. J. Amézquita, M. Y. Quigley, T. Ophelders, J. B. Landis, D. Koenig, E. Munch, and D. H. Chitwood. “Measuring hidden phenotype: Quantifying the shape of barley seeds using the Euler characteristic transform”. In: *in silico Plants* 4.1 (2021), diab033. doi: [10.1093/insilicoplants/diab033](https://doi.org/10.1093/insilicoplants/diab033).
- [2] L. Crawford, A. Monod, A. X. Chen, S. Mukherjee, and R. Rabadán. “Predicting Clinical Outcomes in Glioblastoma: An Application of Topological and Functional Data Analysis”. In: *Journal of the American Statistical Association* 115.531 (2020), pp. 1139–1150. doi: [10.1080/01621459.2019.1671198](https://doi.org/10.1080/01621459.2019.1671198).
- [3] J. Curry, S. Mukherjee, and K. Turner. “How many directions determine a shape and other sufficiency results for two topological transforms”. In: *Transactions of the American Mathematical Society, Series B* 9 (2022), pp. 1006–1043.
- [4] M. Hajij, K. Istvan, and G. Zamzmi. “Cell Complex Neural Networks”. In: “*Topological Data Analysis and Beyond*” Workshop at NeurIPS. 2020. url: <https://openreview.net/forum?id=6Tq18ySFpGU>.
- [5] K. Hornik, M. Stinchcombe, and H. White. “Multilayer feedforward networks are universal approximators”. In: *Neural Networks* 2.5 (1989), pp. 359–366. doi: [10.1016/0893-6080\(89\)90020-8](https://doi.org/10.1016/0893-6080(89)90020-8).
- [6] K. Maggs, C. Hacker, and B. Rieck. “Simplicial Representation Learning with Neural k -forms”. In: *International Conference on Learning Representations*. 2024. url: <https://openreview.net/forum?id=Djw0XhjHZb>.
- [7] E. Munch. *An Invitation to the Euler Characteristic Transform*. 2023. arXiv: [2310.10395](https://arxiv.org/abs/2310.10395) [cs.CG].
- [8] T. Papamarkou, T. Birdal, M. Bronstein, G. Carlsson, J. Curry, Y. Gao, M. Hajij, R. Kwitt, P. Liò, P. D. Lorenzo, V. Maroulas, N. Miolane, F. Nasrin, K. N. Ramamurthy, B. Rieck, S. Scardapane, M. T. Schaub, P. Veličković, B. Wang, Y. Wang, G.-W. Wei, and G. Zamzmi. “Position: Topological Deep Learning is the New Frontier for Relational Learning”. In: *Proceedings of the 41st International Conference on Machine Learning*. Ed. by R. Salakhutdinov, Z. Kolter, K. Heller, A. Weller, N. Oliver, J. Scarlett, and F. Berkenkamp. Proceedings of Machine Learning Research 235. PMLR, 2024, pp. 39529–39555. url: <https://proceedings.mlr.press/v235/papamarkou24a.html>.
- [9] E. Röell and B. Rieck. “Differentiable Euler Characteristic Transforms for Shape Classification”. In: *International Conference on Learning Representations*. 2024. url: <https://openreview.net/forum?id=M0632iPq3I>.
- [10] J. Schmidhuber. *Annotated History of Modern AI and Deep Learning*. 2022. arXiv: [2212.11279](https://arxiv.org/abs/2212.11279) [cs.NE].
- [11] K. Turner, S. Mukherjee, and D. M. Boyer. “Persistent homology transform for modeling shapes and surfaces”. In: *Information and Inference: A Journal of the IMA* 3.4 (2014), pp. 310–344. doi: [10.1093/imaiai/iaou011](https://doi.org/10.1093/imaiai/iaou011).
- [12] P. Veličković. “Everything is connected: Graph neural networks”. In: *Current Opinion in Structural Biology* 79 (2023), p. 102538. doi: [10.1016/j.sbi.2023.102538](https://doi.org/10.1016/j.sbi.2023.102538).
- [13] D. J. E. Waibel, S. Atwell, M. Meier, C. Marr, and B. Rieck. “Capturing Shape Information with Multi-Scale Topological Loss Terms for 3D Reconstruction”. In: *Medical Image Computing and Computer Assisted Intervention*. Ed. by L. Wang, Q. Dou, P. T. Fletcher, S. Speidel, and S. Li. Cham, Switzerland: Springer, 2022, pp. 150–159. doi: [10.1007/978-3-031-16440-8_15](https://doi.org/10.1007/978-3-031-16440-8_15).